Atomic Motion in Liquid Argon

K. SKÖLD
AB Atomenergi, Studsvik, Sweden
AND
K. E. LARSSON
Royal Institute of Technology, Stockholm, Sweden

(Received 1 December 1966)

The atomic motion in liquid argon at 94°K has been investigated by inelastic scattering of 4.1Å neutrons. Special attention was paid to the collective aspects of the motion, and the observations were therefore confined to momentum transfers κ in the region $1.3<\kappa<3.3$ Å^{-1}, which includes the main peak of the liquid structure factor. The results are compared with various models. These comparisons give strong evidence of collective modes, and an extreme polycrystalline model, in which even the polarization of the phonons is retained, gives the best description of the data. There is also definite evidence of a second Brillouin zone in liquid argon. A dispersion relation is obtained with a slope close to the measured velocity of sound and in good agreement with earlier neutron results. The frequency spectrum has been determined and is compared with the results of a computer calculation by Rahman.

I. INTRODUCTION

MUCH effort is at present devoted to studies of the fundamental properties of the liquid state, and considerable progress has been made over the past ten years. Most of the information has been obtained from neutron-scattering experiments from which, in principle, all space- and time-dependent properties can be derived. Neutron experiments have given evidence of damped vibrations, and the frequency distribution of these has been derived for some hydrogen-containing molecular liquids.[1–3] No such experimental information is yet available for a simple monatomic liquid. Evidence has also been obtained of collective modes in the liquid state, and dispersion relations have been determined in a few cases.[4–7] Some qualitative similarities between the solid and liquid states are thus established, and these have been used as guides in constructing models for the scattering cross section. A model due to Egelstaff,[8] in which reciprocal lattice vectors are assumed, is in reasonable agreement with experiments on several liquids,[9,10] but a recent model put forward by Singwi,[11] in which no such assumption is made, seems to have comparable success.[6,12] Both theories suppose that, in accordance with the viscoelastic theory,[13] the liquid will propagate high-frequency ($\omega \gtrsim 10^{12}$ sec^{-1}) vibrations in a way similar to a solid.

Liquid argon is probably the liquid that is easiest to understand theoretically, as it is monatomic and has a rather well-known interatomic potential. A computer experiment by Rahman[14] also shows that a considerable amount of relevant physical information can be obtained even without actually formulating a liquid theory. Several neutron studies of liquid argon have been reported. Dasannacharya *et al.*[15] interpreted the absence of structure in the inelastic region as an indication of a simple diffusive behavior of the atoms. This was consistent with their observation that the experimentally determined mean-square displacement was in good agreement with the predictions of Fick's law for diffusion. Chen *et al.*,[7] on the other hand, observed pronounced structure in the spectra from liquid argon and interpreted this as strong evidence of phonons. No structure was observed in the spectra observed by Kroo *et al.*,[4] but the existence of phonons was made evident by comparing the data with the polycrystalline theory suggested by Egelstaff, and a dispersion relation was derived. A possible explanation of the discrepancies described above is that Chen *et al.* used 5.3 Å neutrons, while the other experiments were made with 4.1 Å incident neutrons. The observed spectra, in which both energy and wave vector change simultaneously, are therefore not directly comparable, and the spectra are, for the same reason, not easily interpreted in terms of dynamical properties. It was

[1] P. A. Egelstaff, in *Proceedings of the Chalk River Symposium on Inelastic Scattering of Neutrons in Solids and Liquids* (International Atomic Energy Agency, Vienna, 1963), Vol. I, p. 65.
[2] K. E. Larsson and U. Dahlborg, Physica **30**, 1561 (1964).
[3] V. V. Goilkov, I. Zukowska, F. L. Shapiro, A. Szkatula, and J. Janik, in *Proceedings of the Bombay Symposium on Inelastic Scattering of Neutrons in Solids and Liquids* (International Atomic Energy Agency, Vienna, 1965), Vol. II, p. 201.
[4] N. Kroo, G. Borgonovi, K. Sköld, and K. E. Larsson, in *Proceedings of the Bombay Symposium on Inelastic Scattering of Neutrons in Solids and Liquids* (International Atomic Energy Agency, Vienna, 1965), Vol. II, p. 101.
[5] S. J. Cocking and P. A. Egelstaff, Phys. Letters **16**, 130 (1965).
[6] P. D. Randolph and K. S. Singwi, Phys. Rev. **152**, 99 (1966).
[7] S. H. Chen, O. J. Eder, P. A. Egelstaff, B. C. G. Haywood, and F. J. Webb, Phys. Letters **19**, 269 (1965).
[8] P. A. Egelstaff, Atomic Energy Research Establishment Report No. AERE-R4101, 1962 (unpublished).
[9] S. J. Cocking and Z. Guner, in *Proceedings of the Chalk River Symposium on Inelastic Scattering of Neutrons in Solids and Liquids* (International Atomic Energy Agency, Vienna, 1963), Vol. I, p. 227.
[10] K. E. Larsson and U. Dahlborg, Arkiv Physik (to be published).
[11] K. S. Singwi, Physica **31**, 1257 (1965).
[12] K. S. Singwi and G. Feldmann, in *Proceedings of the Bombay Symposium on Inelastic Scattering of Neutrons in Solids and Liquids* (International Atomic Energy Agency, Vienna, 1965), Vol. II, p. 85.
[13] J. Frenkel, *Kinetic Theory of Liquids* (Oxford University Press, Oxford, England, 1946).
[14] A. Rahman, Phys. Rev. **136**, A405 (1964).
[15] B. A. Dasannacharya and K. R. Rao, Phys. Rev. **137**, A417 (1965).

shown by Rahman[14] that the frequency spectrum of the velocity autocorrelation function is very sensitive to the exact shape of the mean-square displacement as a function of time, and that even a small deviation from the simple diffusion result will have a drastic influence on the frequency spectrum. The observation of Dasannacharya that the mean-square displacement is, within experimental errors, consistent with simple diffusive behavior should therefore not be taken as serious evidence against the phonon picture.

We have carried out a detailed study of the scattering from liquid argon at 94°K with special attention paid to the wave-vector dependence of the intensity at constant energy transfer. This representation, which clearly displays the interference part of the cross section, is convenient when discussing the collective aspects of the motion. Section II of this report contains a brief review of relevant theories, experimental details are described in Sec. III, and the experimental results are presented in Sec. IV. The data are discussed in Sec. V, where the details of the analysis and the comparison of the experimental data with various models are also described. The results are summarized and conclusions are drawn in Sec. VI. Only inelastic scattering is considered in this report. Small-energy-transfer scattering will be discussed in a second paper.

II. THEORY

A review of theoretical models that are being currently used in the analysis of neutron-scattering results on liquids has recently been given by Sjölander.[16] We shall give a brief outline of those models of which use is made in this paper, and the reader is referred to the article cited above for details.

Van Hove[17] expressed the cross sections as Fourier transforms of certain correlation functions:

$$\frac{d^2\sigma_i}{d\Omega d\omega} = a_i^2 \frac{k}{k_0} \iint \exp[i(\boldsymbol{\kappa}\cdot\mathbf{r}-\omega t)] G_s(\mathbf{r}, t)\, d\mathbf{r}dt, \quad (1)$$

and

$$\frac{d^2\sigma_c}{d\Omega d\omega} = a_c^2 \frac{k}{k_0} \iint \exp[i(\boldsymbol{\kappa}\cdot\mathbf{r}-\omega t)] G(\mathbf{r}, t)\, d\mathbf{r}dt, \quad (2)$$

where all notations have their usual meanings.

Vineyard[18] derived an expression for the coherent cross section on the assumption that the motion of the other atoms is not influenced by the conditioned presence of an atom at the origin at $t=0$. Making this assumption he could express $G(\mathbf{r}, t)$ as

$$G(\mathbf{r}, t) = G_s(\mathbf{r}, t) + \int G_s(\mathbf{r}-\mathbf{r}', t) g(\mathbf{r}')\, d\mathbf{r}', \quad (3)$$

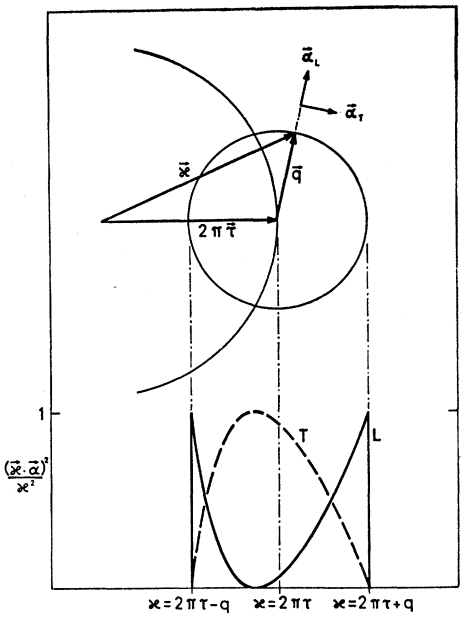

FIG. 1. Vector diagram for a coherent one-phonon process in a polycrystal and the resulting polarization factors.

where $g(\mathbf{r})$ is the pair distribution function. This "convolution approximation" is probably not too bad except for atoms in the nearest-neighbor shells at small times. The most serious formal objections against it have been that it violates the moment relations derived by Placzek[19] and others and that it gives the wrong hydrodynamic limit for small momentum transfer.

Rahman solved numerically the equations of motion for 864 argon atoms with a density corresponding to the liquid state and assumed to interact according to a Lennard-Jones potential. From these calculations he obtained G_s and G_d separately, and he also evaluated G_d from Eq. (3) using the computed G_s and $g(r) = G_d(r, 0)$. It was observed that Vineyard's approximation gave a too rapid decay of the initial structure, given by $g(r)$, and that it could be improved by delaying the convolution. By matching G_d from the delayed convolution with the directly computed G_d he obtained a relation between the actual t and the delayed t at which G_s in the convolution integral should be taken. The delay varies with t and is, for example, 0.6×10^{-12} sec when t is 1.6×10^{-12} sec.

Singwi[11] assumed that all terms in the intermediate scattering function that contain position vectors of atoms more than a certain distance R apart could be treated according to the convolution approximation. Correlated motions of atoms closer than this distance to each other were treated as if the liquid were a quasiharmonic solid. The region within which the

[16] A. Sjölander, *Thermal Neutron Scattering*, edited by P. A. Egelstaff (Academic Press Inc., New York, 1965), p. 291.
[17] L. Van Hove, Phys. Rev. **95**, 249 (1954).
[18] G. H. Vineyard, Phys. Rev. **110**, 999 (1958).
[19] G. Placzek, Phys. Rev. **86**, 377 (1952).

harmonic approximation is applied is limited by introducing a smooth exponential damping of the correlation between equilibrium positions of pairs of atoms. The size of the region is determined by the parameter R. The formula obtained for the one-phonon scattering cross section is

$$\frac{d^2\sigma}{d\Omega d\omega} = a_c^2 \frac{k}{k_0} \exp\left(-\frac{\hbar\omega}{2kT}\right) S^R(\kappa, \omega), \tag{4}$$

where

$$S^R(\kappa, \omega) = S_i^1(\kappa, \omega)\left[\frac{a_i^2}{a_c^2} + S(\kappa) + \operatorname{sech}\left(\frac{\hbar\omega}{2kT}\right)\frac{q^2}{6} L(R, \kappa, q)\right],$$

$$S_i^1(\kappa, \omega) = \exp(-a\kappa^2) \coth\left(\frac{\hbar\omega}{2kT}\right)\frac{\hbar\kappa^2}{4M\omega} f(\omega),$$

$$L(R, \kappa, q) = \frac{3R}{q^2\kappa\pi^{1/2}} \int_0^\infty k[S(\kappa) - 1]\, dk (2q)^{-1}$$

$$\times \int_{-q}^{+q} \{\exp[-(R^2/4)(\kappa - k + x)^2] - \exp[-(R^2/4)(\kappa + k + x)^2] - \exp[-(R^2/4)(\kappa - k)^2] - \exp[-(R^2/4)(\kappa + k)^2]\}\, dx.$$

In writing down this, it has been assumed that the dispersion relation is linear.

It is seen from Eq. (4) that the cross section for a certain ω and κ may be calculated only if the following quantities are known: (a) the scattering lengths a_i and a_c, (b) the Debye-Waller exponent a, (c) the structure factor $S(\kappa)$, (d) the correlation range R, (e) the magnitude q of the phonon wave vector, (f) the frequency spectrum $f(\omega)$.

It was shown by Weinstock[20] that one-phonon coherent scattering from a polycrystal can occur only if κ fulfills the condition

$$2\pi\tau - q \leq \kappa \leq 2\pi\tau + q, \tag{5}$$

where q is the wave number corresponding to the phonon in question and τ is an arbitrary reciprocal lattice vector. Egelstaff[8] suggested the one-phonon coherent scattering in a liquid can be described in the same way as the scattering from a polycrystal if the discrete reciprocal-lattice distances are replaced by the liquid structure factor. $S(\kappa)$ is thus interpreted as the distribution of magnitudes of reciprocal-lattice vectors. Phonon wave vectors can in this case have their origin at any point in reciprocal space, and the scattering picture is obtained after folding $S(\kappa)$ with the phonon distributions described by Eq. (5). The expression for the scattering cross section, including both coherent and incoherent one-phonon scattering, is

$$(d^2\sigma/d\Omega d\omega) = a_c^2 \exp[-(\hbar\omega/2kT)] S^R(\kappa, \omega), \tag{6}$$

where

$$S^R(\kappa, \omega) = S_i^1\left[\frac{a_i^2}{a_c^2} + (2\kappa q)^{-1}\int_{\kappa-q}^{\kappa+q} x S(x) P^j(x, q, \kappa)\, dx\right].$$

S_i^1 is defined in Eq. (4), and the polarization factor $P^j(x, q, \kappa)$ is

$$P^L(x, q, \kappa) = (\boldsymbol{\kappa}\cdot\boldsymbol{\alpha}_L)^2/\kappa^2 \quad \text{(longitudinal phonons)},$$
$$P^T(x, q, \kappa) = (\boldsymbol{\kappa}\cdot\boldsymbol{\alpha}_T)^2/\kappa^2 \quad \text{(transverse phonons)}, \tag{7}$$

where $\boldsymbol{\alpha}_L$ and $\boldsymbol{\alpha}_T$ are unit vectors parallel and at right angles, respectively, to the phonon wave vector. It is assumed that the transverse branches are degenerate, P^j is in the general case the sum of P^L and P^T. The polarization factors have some features of interest. P^L gives a contribution which has a minimum where $S(\kappa)$ has a peak, while P^T is peaked at the maxima of $S(\kappa)$. Together they add up to a smooth peak without structure. The vector diagram which must be fulfilled by $\boldsymbol{\kappa}$, $\mathbf{q}$, and $\boldsymbol{\tau}$ is shown in Fig. 1, where the resulting polarization factors are also shown. Figure 1 refers to the polycrystalline case where the τ vectors have discrete values but are randomly oriented.

Independent of all models, the cross section may be written in terms of the scattering law $S(\kappa, \omega)$ as

$$d^2\sigma/d\Omega d\omega = a^2(k/k_0) S(\kappa, \omega). \tag{8}$$

General expressions for the energy moments of $S(\kappa, \omega)$ were derived by Placzek[19] and later for classical systems by de Gennes.[21] The nth moment is defined as

$$\langle\omega^n\rangle = \int_{-\infty}^{\infty} \omega^n S(\kappa, \omega)\, d\omega. \tag{9}$$

The first three moments are

$$\langle\omega_i^0\rangle = 1,$$
$$\langle\omega_c^0\rangle = S(\kappa),$$
$$\langle\omega_i^1\rangle = \langle\omega_c^1\rangle = -\hbar\kappa^2/2M,$$
$$\langle\omega_i^2\rangle = \langle\omega_c^2\rangle = \kappa^2 kT/2M, \tag{10}$$

[20] R. Weinstock, Phys. Rev. **65**, 1 (1954).

[21] P. D. De Gennes, Physica **25**, 825 (1959).

where in the last line a quantum correction, which should be small for liquid argon, has been neglected. De Gennes obtained the following classical expressions for the 4th moments:

$$\langle\omega_i^4\rangle=3\langle\omega^2\rangle^2+\langle\omega^2\rangle\Omega_0^2,$$
$$\langle\omega_c^4\rangle=3(\langle\omega^2\rangle^2/\langle\omega_c^0\rangle)+\langle\omega^2\rangle\Omega^2, \quad (11)$$

where, if $V(r)$ is the pair potential,

$$\Omega_0^2=M^{-1}\int d\mathbf{r}g(r)\frac{\partial^2}{\partial x^2}V(r), \quad (12)$$

$$\Omega^2=\frac{\kappa^2}{M}\left[3kT\left(1-\frac{1}{S(\kappa)}\right)+\int d\mathbf{r}g(r)\frac{1-\cos\kappa x}{\kappa^2}\frac{\partial^2 V}{\partial x^2}\right]. \quad (13)$$

Ω_0^2 is a constant, while Ω^2 is, in general, a function of κ.

Argon scatters neutrons both coherently and incoherently, so we define the nth moment of the scattering law as

$$\langle\omega^n\rangle=\tfrac{1}{3}\langle\omega_i^n\rangle+\tfrac{2}{3}\langle\omega_c^n\rangle, \quad (14)$$

where the coefficients are obtained by assuming that $a_c^2/a_i^2=2$, which is the ratio obtained by Henshaw.[22]

Combining Eqs. (11) and (14), we obtain a relation between Ω, Ω_0, and the observed moments:

$$\Omega_0^2+2\Omega^2=3(\langle\omega^4\rangle/\langle\omega^2\rangle)-\langle\omega^2\rangle[3+(12/3\langle\omega^0\rangle-1)]. \quad (15)$$

This combination of the squares of the characteristic frequencies is all one can determine experimentally unless the coherent and incoherent contributions to the scattering law are separated.

III. EXPERIMENTAL DETAILS

The experiment was carried out using the cold-neutron time-of-flight spectrometer at the R2 reactor in Studsvik. A detailed description of this instrument is given elsewhere[23] and we shall therefore give an account of the most important features only.

The reactor beam is filtered through 20 cm of Bi and 50 cm of Be, both cooled to liquid-nitrogen temperature, before it is chopped by a semimonochromating chopper placed in front of the sample. This filter-chopper combination produces an incident spectrum with an average energy of 4.9 meV and a full width at half-maximum of 0.9 meV. Spectra are recorded at two angles simultaneously on a 1024-channel time analyzer provided with a four-detector input unit. Each of the two detector banks now in use consists of 18 BF_3 counters arranged in one layer. The detector tubes are 30 mm in diameter and filled with BF_3 gas, enriched to 90.5% in B^{10}, to a pressure of 1500 mm Hg. Both flight paths, 460 cm long, are evacuated over most of their lengths, leaving only 1.4 m of air between the sample and the detector. The angular spread of the scattered beam is about 4°, while the collimation before the sample is about 1°. The energy resolution of the scattered spectrum is better than 3% everywhere between 3 and 12 meV, which is the energy range of interest in this study. The uncertainties in the energy transfers are thus essentially due to the width of the incident spectrum, while the uncertainties in the wave-vector transfers are due to the combined effect of the angular spread of the scattered beam and the width of the incident spectrum.

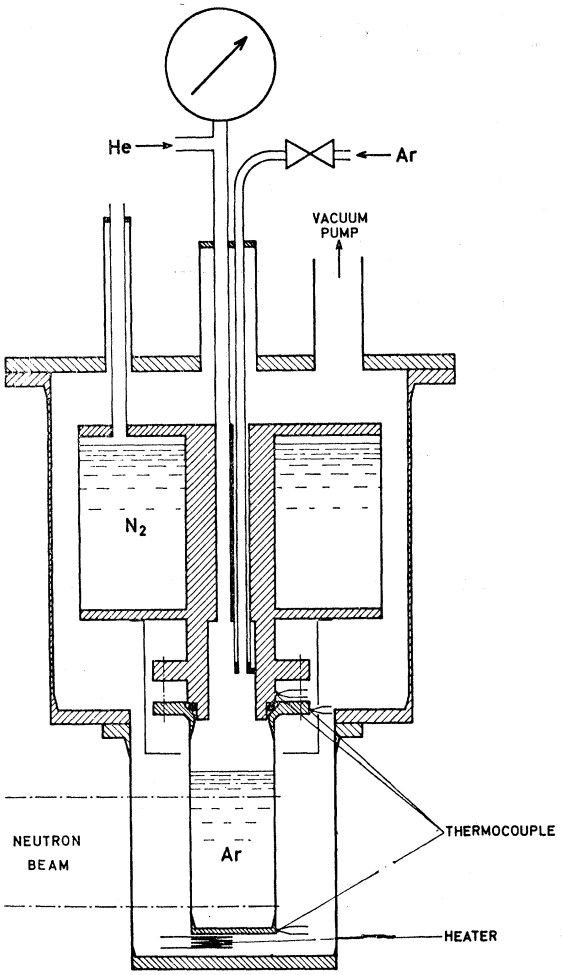

FIG. 2. Sample arrangement.

A drawing of the cryostat in which the sample was contained is shown in Fig. 2. The argon container is made of aluminum in the form of a cylinder with diameter 6 cm and wall thickness 0.1 cm. The cryostat was cooled with liquid nitrogen. The heating required to reach the appropriate temperatures for measurements on liquid argon was supplied by an electric heater attached to the bottom of the scattering cham-

[22] D. G. Henshaw, Phys. Rev. **105**, 976 (1957).
[23] S. Holmryd, K. Sköld, E. Pilcher, and K. E. Larsson, Nucl. Instr. Methods **27**, 61 (1964).

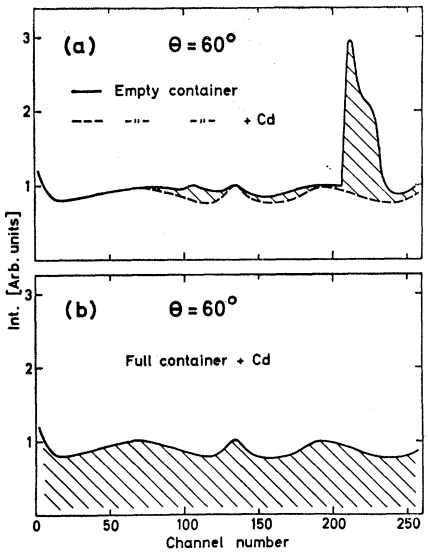

FIG. 3. Examples of spectra used to determine the total background.

ber. Temperatures below the normal boiling point of nitrogen, necessary for some of the measurements on solid argon, were reached by pumping on the coolant. The temperature of the sample was measured with three thermocouples placed at the bottom, at the top, and above the container, respectively. It was assumed that the temperature gradient over the sample could be obtained from the difference of the readings of the thermocouples at the bottom and at the top of the argon chamber and that the average temperature of the sample was equal to the average of these readings. We believe that the temperature of the active part of the sample is safely within the limits obtained in this way. Fluctuations in temperature were much smaller than the gradients and are therefore neglected when quoting the errors.

The liquid was kept under its own vapor pressure, which was always higher than 1 atm. In this way we avoided contamination with air, which could otherwise leak in to the sample and accumulate there over long periods. No difference was observed between spectra taken with a fresh sample and with one that had been kept in the cryostat for 3 weeks, which is about the longest time one sample was used. When measuring on solid argon we used He gas at a pressure of 1.2 atm as a cover above the solid surface.

Two types of background runs were made. One background was taken with the sample container filled and with a sheet of Cd shielding the sample volume away from the detector. Such a spectrum includes all the background except the component consisting of thermal neutrons scattered by extraneous material around the sample. This latter component was determined by taking the difference between the spectrum observed from the empty container and the spectrum obtained with the empty container shielded by the Cd sheet. Examples of the three types of spectra that were used in the background correction are shown in Fig. 3. The total background was obtained by adding together the hatched areas in Figs. 3(a) and 3(b). This procedure includes the assumption that there are no thermal background neutrons scattered by the sample itself. As most of the beam path in the sample area was lined with Cd, and the incident beam contains very few thermal neutrons that have leaked past the chopper, this assumption should be rather safe. The disturbance from neutrons first scattered by the sample and then by material around the sample was diminished by lining the inner wall of the vacuum container with Cd, leaving only the necessary openings for the incident and scattered beams. The reason why the spectrum from the empty container was not considered a good representation of the total background is that the incident beam is contaminated with fast neutrons, and these are scattered more efficiently with the container filled. The effect is most pronounced at small scattering angles and not observable at all for the larger angles, where in many cases only the empty-container background was used. One reason to be particularly careful with the fast-background correction is that the intensity of fast neutrons coming through the chopper is modulated. This modulation, which is there because the rotor has different stopping power in different orientations, is clearly visible in Fig. 3. The relative importance of the background correction can be seen from Fig. 4, where examples of backgrounds are shown together with the intensities observed with a full container at the corresponding angles. After sub-

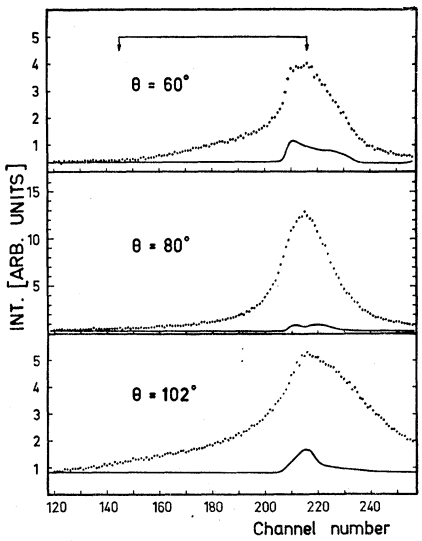

FIG. 4. Spectra obtained with full container shown together with total backgrounds at small, medium, and large scattering angles. Arrows show the limits within which data used in the analysis were taken.

tracting the background as described above, the data were corrected for the energy-dependent loss of neutrons by air scattering in those parts of the flight path that were not evacuated. The data were finally corrected for the energy-dependent efficiency of the detectors and converted from the time-of-flight to the frequency scale.

Most of the analysis of these data was concerned with the variation of the intensity with wave-vector transfer, and it was therefore important that runs taken at different angles were properly normalized. This was accomplished by using two detectors and moving only one at a time. The runs were normalized by ensuring that the ratio between the normalized total intensities at two angles was the same as the ratio between the intensities observed in simultaneous runs at these angles. This method was considered preferable to one based on monitoring the incident flux because it was difficult to check if the container were filled to the same level all the time. The procedure that was used is a normalization to the same incident flux and to the same number of scattering atoms.

No correction was applied for multiple-scattering events, mainly because this correction should be rather small, but also because we do not know any simple and reliable way to perform it. The transmission of the sample for 4 Å neutrons was 93%, and the sample had the form of a cylinder, which, we believe, is a favorable shape in this connection.

IV. PRESENTATION OF DATA

Spectra scattered from liquid argon at $(94\pm2)°K$ were recorded at 17 scattering angles ranging from 50° to 130°. Examples of the raw data at small, medium, and large scattering angles, respectively, are given in Fig. 4, where the corresponding total backgrounds are also shown (solid curves). The region of the energy transfer within which data were used in the analysis is marked by arrows in Fig. 4, where it is seen that the background correction is rather important at the largest energy transfers considered. All 17 spectra are shown in Fig. 5 with backgrounds subtracted and with all the other corrections that were described above performed, but with no correction for the width of the incident spectrum. The spectra are shown as functions of ω_1, which is the final neutron frequency. The absolute value of the cross section was obtained from a consideration of the energy moments of the scattering law. This normalization is described below.

The shape of the incident spectrum, which is shown in the upper part of Fig. 5, is seen to have a width comparable to the widths of the scattered spectra. These are therefore not true representations of the cross section unless the effect of the incident distribution is corrected for. This correction is important for small energy transfers only, however.

A large part of the analysis is concerned with the coherent scattering, and the most convenient representation of the data is therefore one in which the energy (or frequency) transfer is kept constant and the wave-vector transfer is allowed to vary. The data are shown in this way in Fig. 6 for the frequencies marked by arrows in Fig. 5. The corresponding frequency transfers are given in Fig. 6. Figures 7 and 8 show the result of measurements on solid and liquid argon at various temperatures. These spectra are not normalized to each other, but displayed in the most convenient way for a comparison of the shapes. Spectra observed at 60° scattering angle from liquid argon at 94 and 102°K and from solid argon at 68 and 78°K are shown in Figs. 7(a) and 7(b), respectively. The scattering from solid argon is compared with the scattering from liquid argon in Fig. 8(a) for $\theta=60°$ and in Fig. 8(b) for $\theta=102°$. The data shown in Figs. 7 and 8 are corrected for background only.

V. DISCUSSION

Analyses of neutron scattering results on liquids are often made along lines that are well defined for solids but are not easily based on first principles for liquids. In cases where the scattering is very similar for the two phases this procedure seems reasonable, and the modified polycrystalline theories described above have in fact been successfully applied to several liquids.[9,10] Among the materials that have been studied aluminum[10] is perhaps the one showing the most striking similarity between the spectra scattered from the solid and the liquid phase. From a first glance at the spectra from liquid argon, shown in Fig. 5, where no sharp rises or falls of the intensity are visible, one would be inclined to believe that polycrystalline models are not adequate in this case. This conclusion seems to find support in Figs. 8(a) and 8(b) where examples of the scattering from solid and liquid argon are shown. The spectra from the individual phases at various temperatures are compared in Figs. 7(a) and 7(b), where it is seen that the inelastic spectrum scattered from a single phase is rather insensitive to variations of temperature. We must therefore conclude that the most significant change of the spectrum occurs at the phase transition. It is, however, seen from Fig. 8 that spectra scattered from the two phases, although very different at small energy transfers, are rather similar at large energies. If it is assumed that the liquid spectrum can be separated into a quasielastic part and an inelastic part, and if the quasielastic contribution, assumed to be Lorentzian in shape, is subtracted, we are left with an inelastic spectrum which is not very different from the one scattered from solid argon. This procedure involves some rather arbitrary assumptions, and we are therefore not making any quantitative use of it, but only conclude that the main difference between the scattering from solid and liquid argon can be qualita-

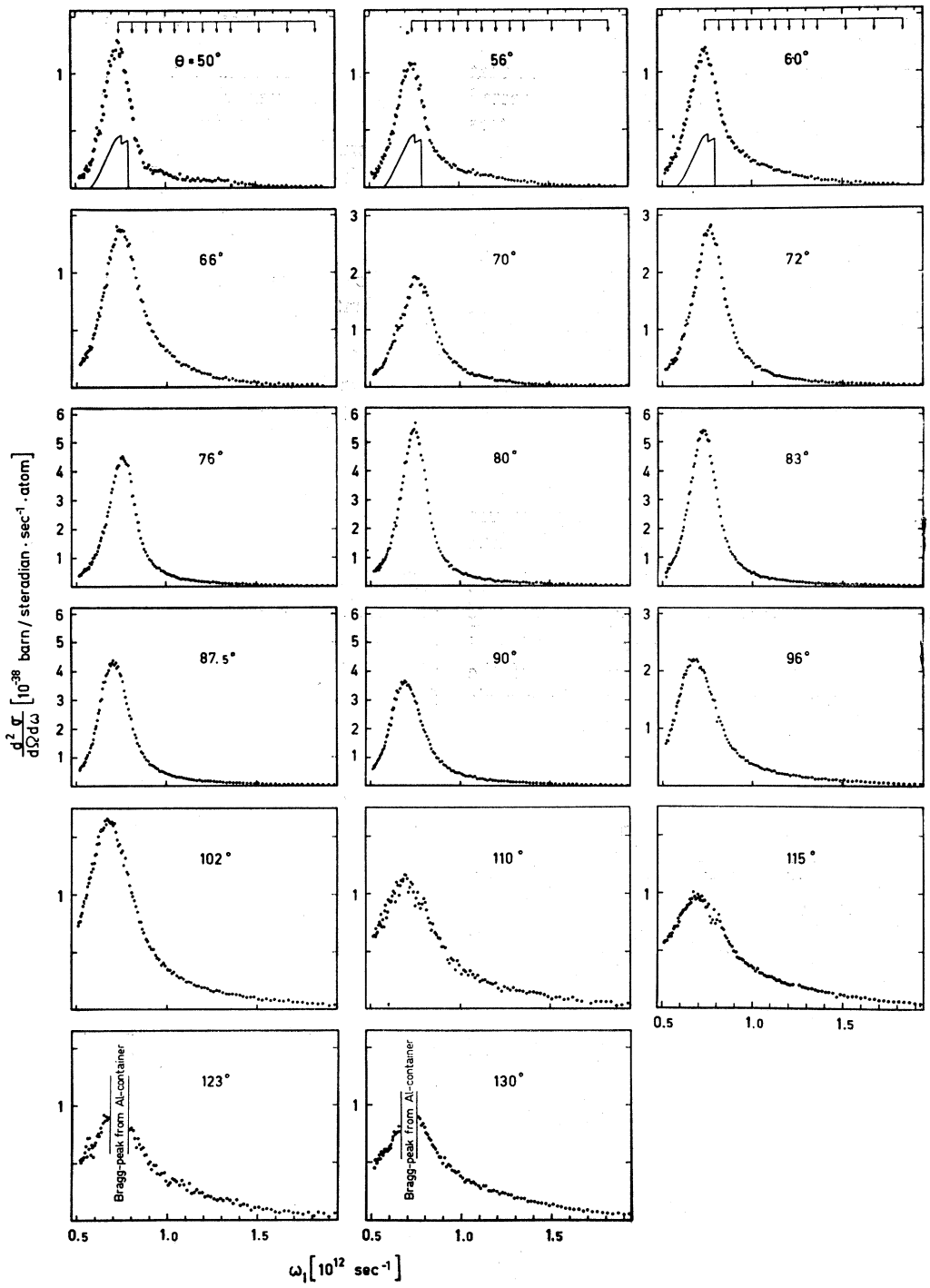

FIG. 5. Finally corrected spectra at 17 scattering angles versus final neutron frequency. The incident spectrum is shown in the upper part of the figure, where the frequencies at which constant-frequency plots were made (see Fig. 6) are shown by arrows.

tively explained by the presence of diffusion in the liquid. Diffusion will give rise to quasielastic scattering but does not necessarily have a drastic influence on the vibratory motion. We may therefore try to explain the inelastic scattering from liquid argon in terms of phonons as long as not-too-small energy transfers are considered.

The observed cross section is shown as a function of κ for several values of the frequency transfer in Fig. 6, from which some general conclusions may be drawn.

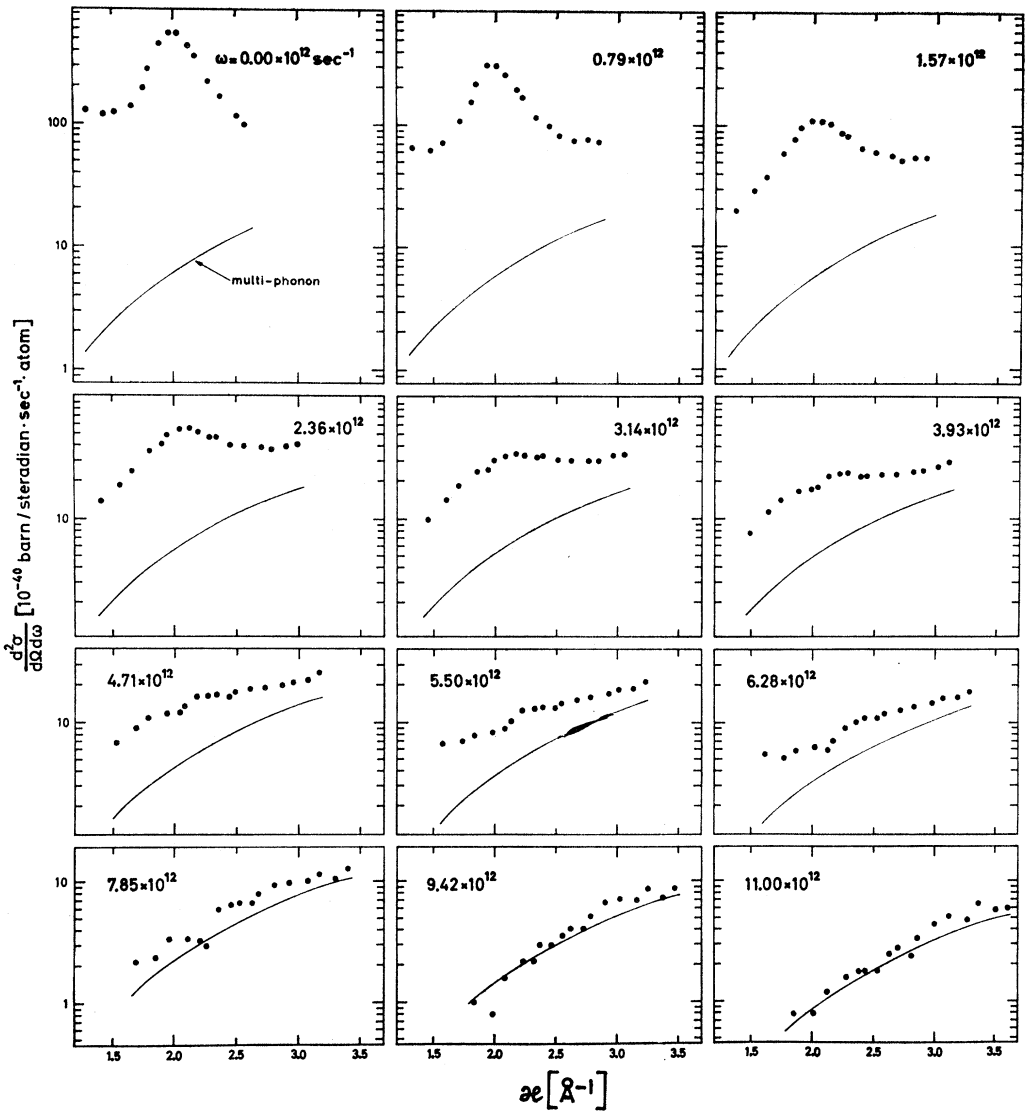

FIG. 6. The cross section at various frequency transfers shown as a function of κ. Full lines show the multiphonon term calculated from Sjölander's formula.

The structure is very similar to that of $S(\kappa)$ for small values of the frequency transfer. Most of the data are in the region of the first peak of $S(\kappa)$, and it is seen how this peak broadens as ω increases and how for large values of ω a minimum develops where $S(\kappa)$ has its most pronounced maximum. This behavior is completely inconsistent with the convolution approximation, which predicts that the first diffraction peak should persist as the energy transfer increases. The decay of the initial structure is, on the other hand, predicted by the models of Singwi and Egelstaff. These models will be given detailed consideration below.

The theoretical cross sections [Eqs. (4) and (6)] contain one-phonon terms only, and we must therefore correct our data for multiphonon contributions before they are compared with the formulas. Higher phonon terms were computed from Sjölander's multiphonon expansion.[24] The correctness of the incoherent approximation for the multiphonon terms for a coherent scatterer has been experimentally proved for the case of a single crystal of aluminum.[25] The frequency-distribution function $f(\omega)$, which is needed in this calculation, was assumed to be a Debye spectrum with $\Theta_D = 50°K$, which is the Debye temperature for liquid argon evaluated from the known value for the solid[26] (81°K) and Mott's relation.[27] The use of a more realistic ex-

[24] A. Sjölander, Arkiv Physik **14**, 315 (1958).
[25] K. E. Larsson, S. Holmryd, and U. Dahlborg, in *Proceedings of the Vienna Symposium on Inelastic Scattering of Neutrons in Solids and Liquids* (International Atomic Energy Agency, Vienna, 1961), p. 587.
[26] N. Bernardes, Phys. Rev. **112**, 1534 (1958).
[27] N. F. Mott, Proc. Roy. Soc. (London) **146**, 465 (1934).

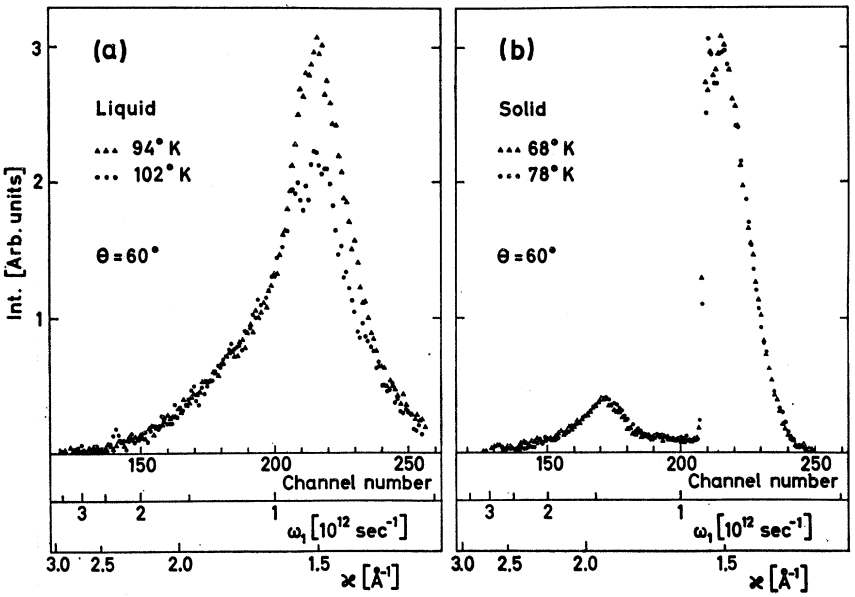

FIG. 7. Spectra scattered at 60° from liquid argon at 94 and 102°K, respectively (a), and from solid argon at 68 and 78°K, respectively (b).

pression for $f(\omega)$, for example the function obtained by Rahman,[14] would not significantly improve these computations, as the multiphonon cross section is rather insensitive to the exact shape of $f(\omega)$. The absolute value of the computed multiphonon intensity depends critically on Θ_D, which is obtained in a rather indirect way, and the normalization was therefore made by assuming that all the intensity at the largest frequency transfer ($\omega=1.1\times10^{13}$) arises from multiphonon events. This normalization, which probably slightly overestimates the multiphonon intensity, is approx. 60% larger than the one calculated with $\Theta_D=50$°K. The normalized curves are shown by the solid lines in Fig. 6, where it is seen that the multiphonon term fits the experimental points rather well at $\omega=1.1\times10^{13}$ sec^{-1}, the normalization frequency.

The cross section including one-phonon terms only is shown in Fig. 9 for various values of the frequency transfer. The error flags show the counting statistics and the triangles show the resolution in κ. Also shown in this figure are the cross sections calculated from Singwi's formula (full curves and dashed curves) for

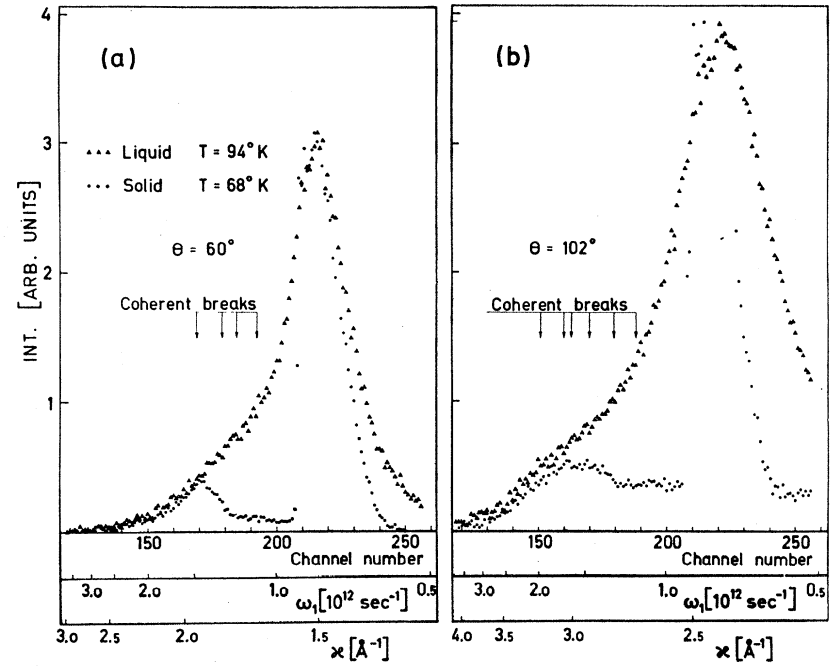

FIG. 8. Spectra scattered at 60° (a) and at 102° (b), from solid argon at 68°K and from liquid argon at 94°K, respectively. Calculated positions of coherent breaks [compare Eq. (5)] are shown by arrows.

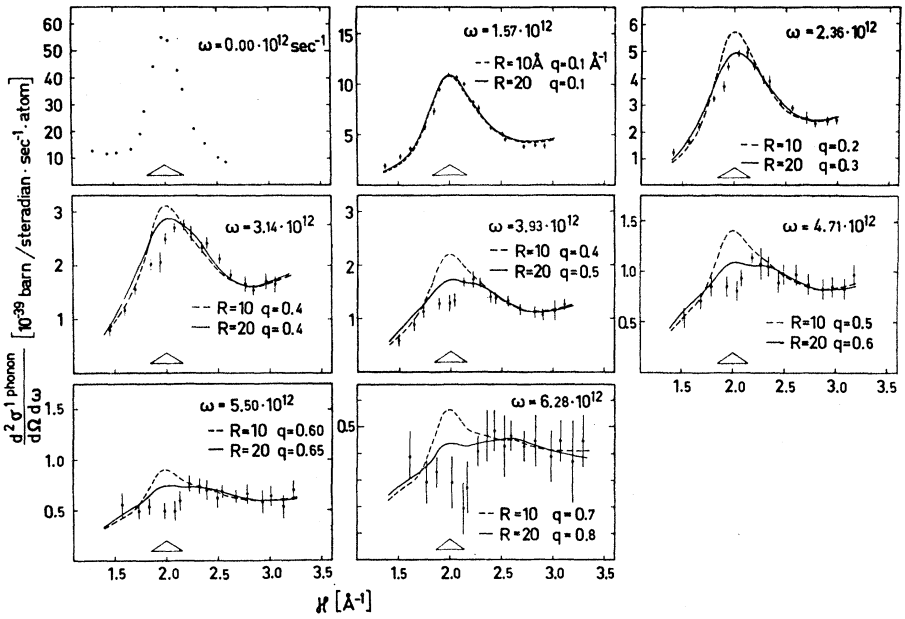

FIG. 9. Experimental one-phonon cross section versus κ at various frequency transfers, shown together with the cross section calculated from Singwi's model. Error flags show the counting statistics, and triangles show the resolution in κ.

those values of R, q, and $f(\omega)$ that gave the best fit. In all these calculations the Debye-Waller exponent was equal to 0.136 Å^2, the ratio a_i^2/a_c^2 was equal to $\frac{1}{2}$, and $S(\kappa)$ was taken from Gingrich's x-ray work.[28] The shape of the cross section depends on the values chosen for R and q, while the variation of the intensity with ω, e.g., from spectrum to spectrum in Fig. 9, is determined by the form of $f(\omega)$. The dependence of the shape on R and q is demonstrated in Fig. 10, where it is seen that the value of q is important, but that the shape is rather insensitive to the value of R when R is larger than about 20 A. After trying various combinations of R and q, we came to the conclusion that R should be not smaller than 10–20 Å. This is all the information we can obtain from the present data about the value of R. A similar conclusion was earlier drawn from a fit of Singwi's model to data on liquid aluminum[10] and liquid lead.[6]

It may be observed from Fig. 9 that when ω increases, a dip develops on the top of the experimental peak at $\kappa=2$ Å^{-1}. This structure is not reproduced by the theoretical curves, which in fact have maxima

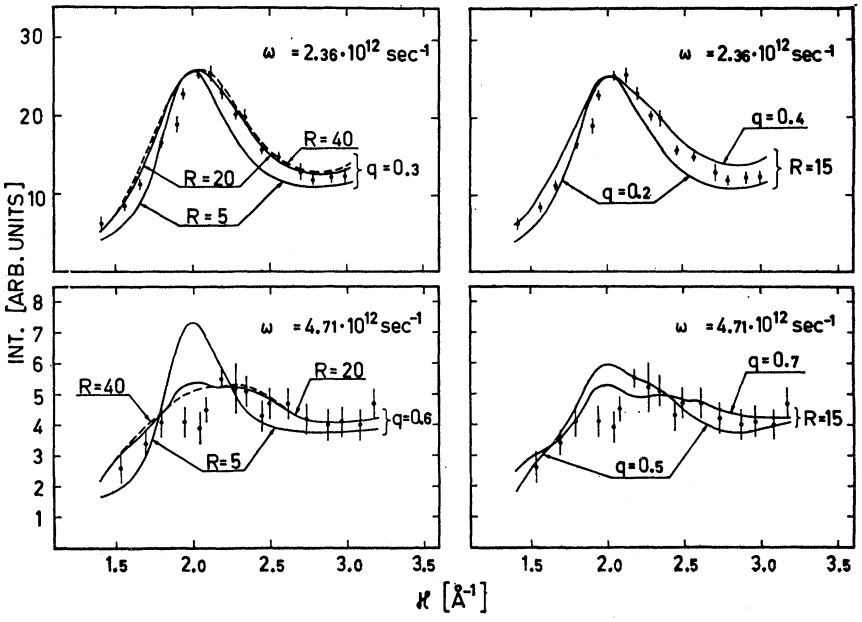

FIG. 10. Effects of varying the parameters R and q on the cross section calculated from Singwi's model.

[28] N. S. Gingrich and C. W. Tompson, J. Chem. Phys. **36**, 2398 (1962).

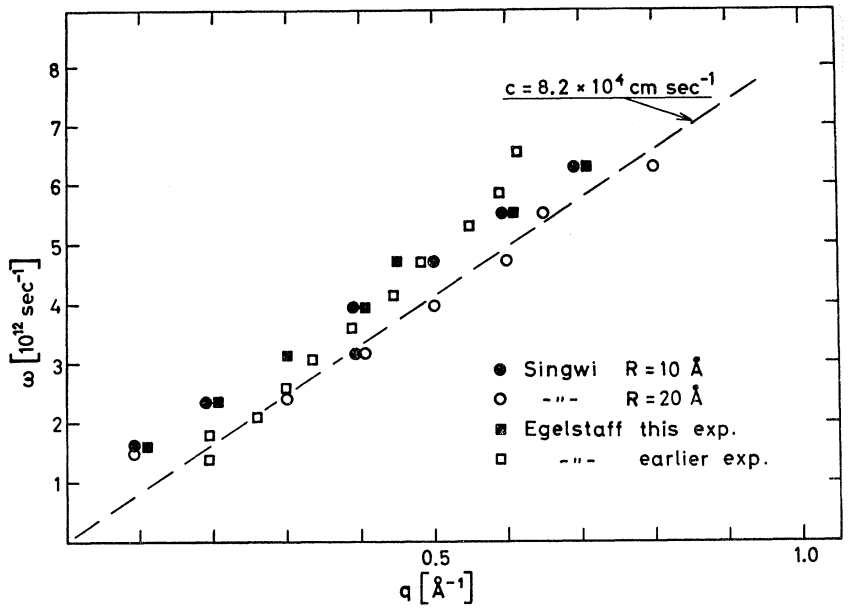

FIG. 11. ω-q relations obtained by applying Singwi's model with $R=10$ Å and $R=20$ Å to the data obtained in this experiment, and the relations obtained by applying Egelstaff's model to the data obtained in this experiment and in the experiment by Kroo. The dashed line shows a linear dispersion curve with $c=8.2\times 10^4$ cm/sec.

instead of minima at this value of κ. We shall discuss this effect below and at this point only remark that we believe that it has its origin in the polarization of the vibrations. These were not given proper consideration in Singwi's treatment, and when fitting his expression to the observations we omitted the region around $\kappa=2.0$ Å^{-1} and used only the wings of the peak. In this way we evaluated the values of q that gave the best fit at each ω with $R=10$ Å and $R=20$ Å, respectively. The pairs of ω and q that were obtained from this analysis are shown in Fig. 11 (filled circles and open circles) where the dashed line is a linear dispersion curve with a slope equal to the velocity of sound in liquid argon at 90.3°K as observed by acoustic methods.[29] The value of R is seen to have a slight influence on the q values. With R and q known, $f(\omega)$ was derived for each ω from the amplitude of the cross section. Figure 12 shows the experimental $f(\omega)$ together with the curve obtained by Rahman. The absolute value of the experimental $f(\omega)$ is about 60% higher than the points shown in Fig. 12, which is plotted in the most convenient way for a comparison of the shapes. Singwi's cross section is probably not adequate at small frequency transfers, and the discrepancy at small frequencies may not be significant. This region is also influenced by the spread in the

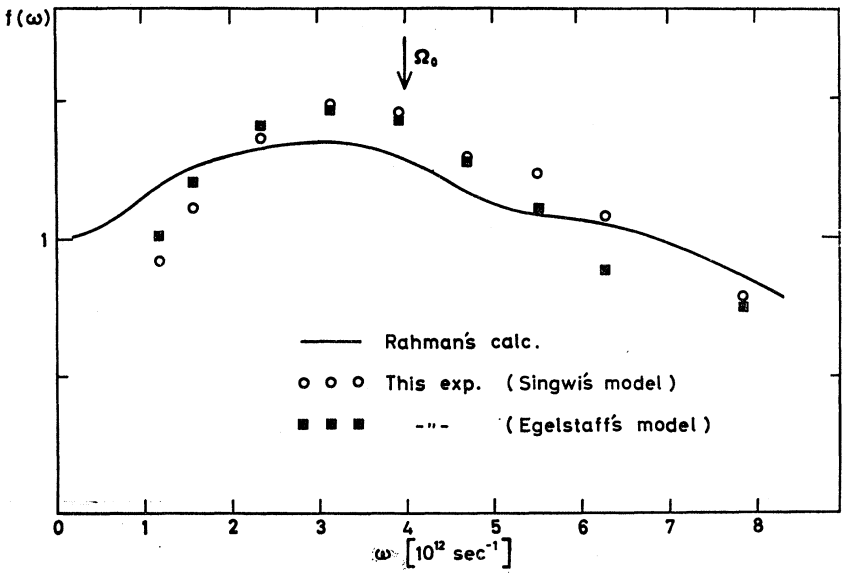

FIG. 12. Experimentally determined $f(\omega)$ compared with the theoretical curve obtained by Rahman. The characteristic frequency obtained by Sears is marked by the arrow.

[29] A. Van Itterbeek, Physica 25, 640 (1959).

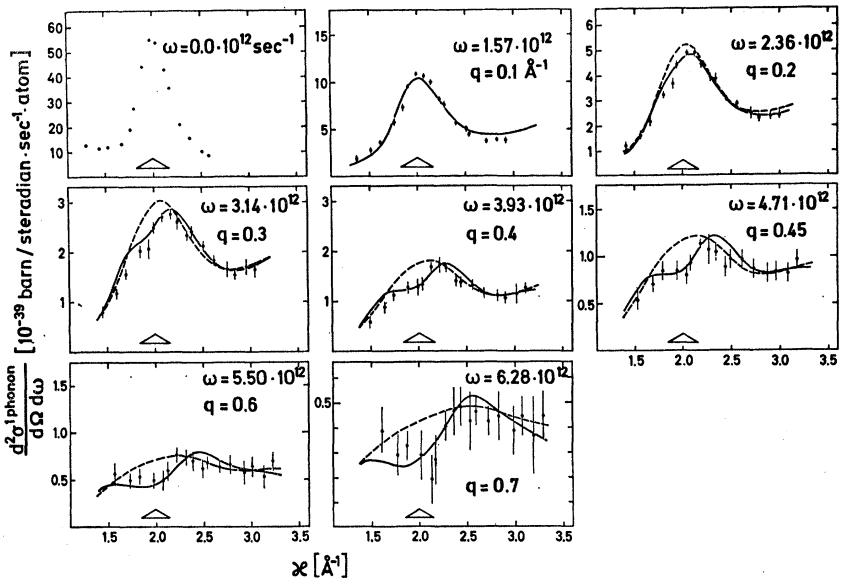

FIG. 13. Experimental one-phonon cross section versus κ at various frequency transfers shown together with the cross section calculated from Egelstaff's model. Dashed curves include both longitudinal and transverse phonons, while solid curves show the cross section obtained if only longitudinal phonons are assumed. Error flags show counting statistics and triangles show the resolution in κ.

incident spectrum, which is not corrected for. It is unfortunate that the data are not reliable in this region of ω, as it would be of interest to know whether the diffusive and vibratory parts of $f(\omega)$ are separated by a dip or not. Such a separation would mean that the two types of motion are not strongly coupled.[16]

Egelstaff's model is on the whole much more solid-like. The thermal motion is described in terms of phonons, and it is assumed that not only the phonons but also the "lattice" can absorb momentum from the neutron. Phonon wave vectors are therefore not necessarily parallel to $\boldsymbol{\kappa}$, and polarization effects must be considered. It is seen from Fig. 1 that a longitudinal phonon gives a contribution which has the form of double peak centered at the origin of the phonon wave vector. Transverse phonons fill up the valley between the peaks, but the resulting distribution will show a dip at the center if the number of transverse phonons is smaller than the number of longitudinal phonons. Structure is also observed if the transverse wave vector is much larger than the longitudinal wave vector. The transverse intensity is in this case spread over a wide region of κ and the dip is not completely filled up.

The observed one-phonon cross section is compared with the cross section calculated from Egelstaff's formula in Fig. 13 for various values of ω. Dashed curves are obtained by assuming both longitudinal and transverse phonons, while full curves show the cross section assuming only longitudinal phonons. $S(\kappa)$, a, and a_i^2/a_c^2 were the same as above. Various values of q, in steps of 0.05 Å^{-1}, were tried for each ω, and the values that gave the best fit are shown in Fig. 13. It is clearly seen that the model in which only longitudinal phonons are included is in much better agreement with the observations than is the model in which both types of phonons contribute. The structure in the region of $\kappa=2$ Å^{-1}, as well as the whole set of experimental points, are in good qualitative, and in fact even quantitative, agreement with the theoretical curve. It would probably be easy to improve this agreement by trying various damping factors for the transverse contribution and by using different wave vectors for longitudinal and transverse phonons. Assuming that the wave vectors at a given frequency are the same, we find that the transverse phonons are almost completely damped for $\omega>3\times10^{12}$ sec^{-1}. The two components give rather similar results for smaller values of q, and therefore no conclusion can be drawn about the existence of transverse vibrations for $\omega<3\times10^{12}$ sec^{-1}, which corresponds to $q<0.25$ Å^{-1}.

The pairs of ω and q that were obtained from this analysis are shown by the filled squares in Fig. 11, where the results of an earlier study by Kroo *et al.*[4] are also shown (open squares). In the experiment by Kroo, only the width of the first diffraction peak—or in fact the width obtained by measuring the intensity for $\kappa\gtrsim2$ Å^{-1} and assuming that the peak is symmetric around $\kappa=2$ Å^{-1}—was used to determine the proper q at a given ω. It will be observed that the frequency–wave-vector relations that were obtained from these two independent studies in which Egelstaff's model was applied and the relation that was obtained by applying Singwi's model agree within the experimental accuracies. This gives strong support to the basic assumption employed in both of these models, that the motion can be described as collective vibrations with well-defined frequencies and wave vectors. The results are also in reasonable agreement with the dispersion curve that is obtained in the Debye model from the measured velocity of sound (dashed line in Fig. 11).

The structure in $S(\kappa, \omega)$ in the neighborhood of the

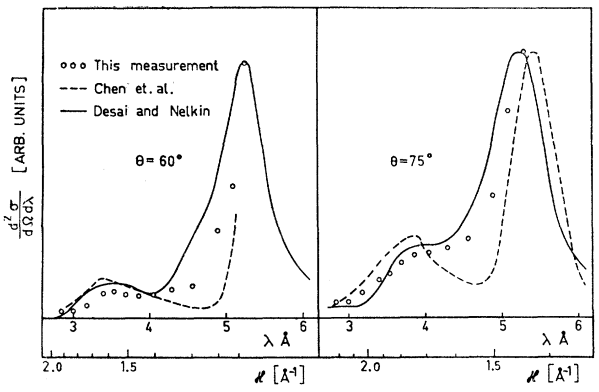

FIG. 14. The cross section calculated by Desai and Nelkin from the delayed-convolution approximation, together with experimental results from this study and from the study by Chen *et al.*

principal diffraction maximum was not discovered in the earlier study of liquid argon, probably because data were not taken close enough in κ and not over the whole peak, and also because the counting statistics were rather bad. However, a similar structure was recently observed in liquid lead by Randolph and Singwi[6] who concluded that it is qualitatively explained by the Singwi model. This is not in accordance with our explanation, where the existence of reciprocal-lattice vectors and the damping of transverse phonons are important ingredients.

The frequency spectrum that was obtained by applying Egelstaff's model is shown by the filled squares in Fig. 12, together with the results obtained by applying Singwi's model. The two results are seen to be in fair agreement, although some minor differences are observed.

Rahman's[14] delayed convolution model, together with the directly computed G functions, was used by Desai and Nelkin[30] to evaluate the scattering cross section, which was compared to the experimental results on liquid argon by Chen *et al.*[7] The calculations were made for an incident wavelength $\lambda_0=5.3$ A and scattering angles equal to 60° and 75°, which are the conditions under which the experiment by Chen was conducted. The calculated spectra are shown in Fig. 14 (solid lines) together with the experimental results by Chen (dashed lines) and the results of this experiment (circles), converted so that they correspond to the same λ_0 and scattering angles. It will be seen that our data are in good qualitative agreement with the delayed convolution results, but the comparison should be made over a larger area of the κ-ω plane before definite conclusions can be drawn about the success of the model. The difference between Chen's results and ours is not understood. It could, at least partly, be due to the fact that the experiments were made at different temperatures (85 and 94°K, respectively), although this would be in contradiction to our observation that the inelastic scattering is rather independent of temperature (compare Fig. 7). Rahman's computer experiment was performed at 94.4°K, which is close to the temperature employed by us.

The reason why structure is observed with 5.3 Å incident neutrons but not with 4.1 Å neutrons is probably only that the wave vector is larger at the same angle in the latter case, so that the diffusion peak is broad enough to fill up the valley between the inelastic and the quasielastic regions (compare observations at 60° in Figs. 8 and 14).

The zeroth, first, second, and fourth moments were obtained by numerical evaluation of the integral in Eq. (9). $S(\kappa, \omega)$ was determined for positive values of ω, and $S(\kappa, -\omega)$ was then obtained from the law of detailed balance:

$$S(\kappa, -\omega)=\exp(-\hbar\omega/kT)\,S(\kappa, \omega). \qquad (16)$$

The gas model was used to extrapolate the integral beyond $\omega=7.8\times10^{12}$ sec^{-1} for all values of κ. Representative integrands for small, medium, and large values of κ are shown in Fig. 15, where $S_T(\kappa, \omega)=S(\kappa, \omega)+(-1)^n S(\kappa, -\omega)$. Extrapolated curves are shown by the dashed lines. The extrapolated fractions of the moments are largest for the largest value of κ, but are everywhere less than 3% for $\langle\omega^0\rangle$, 10% for $\langle\omega^1\rangle$, 8% for $\langle\omega^2\rangle$, and 40% for $\langle\omega^4\rangle$. The gas model should be better applicable as κ gets larger, and this tends to diminish the error introduced by the extrapolation. The experimental $\langle\omega^0\rangle$ is shown by the points in Fig. 16, where the dashed line shows the neutron diffraction results obtained by Henshaw[22] at $T=84$°K. The solid line shows the x-ray data obtained by Gingrich[28] at the same temperature. It will be seen that the two sets of neutron data are in rather good agree-

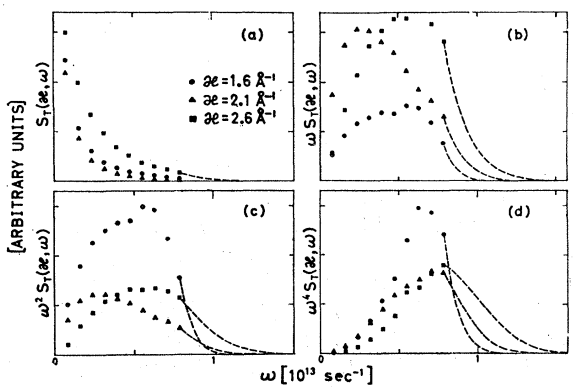

FIG. 15. Representative examples of integrands used in the evaluation of the moments. $S_T(\kappa, \omega)=S(\kappa, \omega)+(-1)^n S(\kappa, \omega)$. Dashed curves show the extrapolated integrands.

[30] R. C. Desai and M. Nelkin, Phys. Rev. Letters **16**, 839 (1966).

ment, but that the x-ray and the neutron results are significantly different. Such discrepancies between x-ray and neutron data have been observed earlier.[6] Absolute values were known only for the x-ray data, and these were therefore used to normalize our experimental $S(\kappa, \omega)$. This was done by normalizing $\langle\omega^0\rangle$ to the same are as $\frac{1}{3}+\frac{2}{3}S(\kappa)_{\text{x ray}}$ over the region 1.6 $\text{Å}^{-1} \leq \kappa \leq 2.6$ Å^{-1}. In this way we obtained the cross section as well as all the other moments in absolute values. In Fig. 17 the experimentally determined moments are compared with the calculated moments. $\langle\omega^0\rangle_{\text{calc}}$ is equal to $\frac{1}{3}+\frac{2}{3}S(\kappa)$ with $S(\kappa)$ taken from Gingrich's work. The calculated first and second moments are obtained from Eqs. (10) and (14), and $\langle\omega^4\rangle_{\text{calc}}$ is taken equal to $3\langle\omega^2\rangle^2$ which is correct only for a Gaussian scattering law. $\langle\omega^1\rangle_{\text{expt}}$ is as much as a factor of 2 smaller than the calculated value in certain regions of κ while $\langle\omega^2\rangle_{\text{expt}}$ and $\langle\omega^4\rangle_{\text{expt}}$ everywhere agrees within 50% with the calculations.

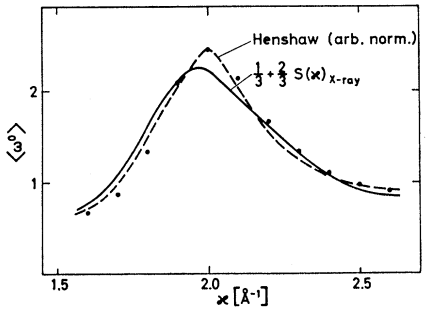

FIG. 16. The zeroth moment obtained in this experiment (dots) compared to the neutron result of Henshaw and the x-ray result of Gingrich.

$(\Omega_0^2+2\Omega^2)$ was evaluated for various values of κ by inserting the observed moments in Eq. (15). The result is shown in Fig. 18, where it will be seen that the function is constant, contrary to the expected κ dependence of Ω. The quantity Ω_0 was calculated by Sears[31] from the frequency spectrum obtained by Rahman[14] and also from Eq. (12). In both cases a value close to 4×10^{12} sec^{-1} was obtained. It was pointed out by Sears that Ω_0 should correspond to the frequency at maximum in $f(\omega)$, and this is seen to be nearly the case from Fig. 12, where the frequency obtained by Sears is shown by the arrow. When the momentum transfer increases, the details of the atomic motion are no longer seen in the scattering process, and therefore the distinction between coherent and incoherent scattering is lost. Therefore $\Omega\to\Omega_0$ when $\kappa\to\infty$, and as Ω seems to be a constant, we may assume that $\Omega=\Omega_0$ everywhere. From this and $\Omega_0^2+2\Omega^2=4\times10^{25}$ sec^{-2} we obtain $\Omega=\Omega_0=3.7\times10^{12}$ sec^{-2}, which

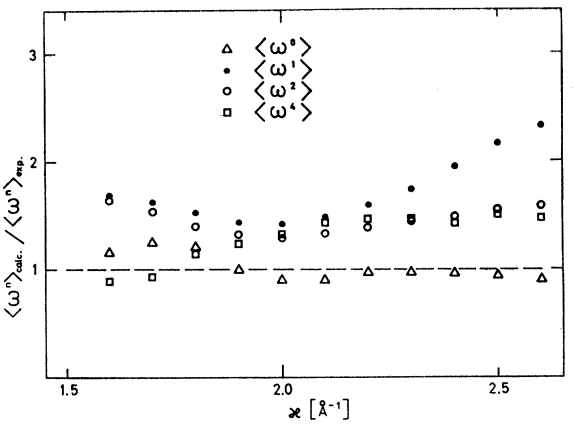

FIG. 17. Ratio of theoretical and experimental moments at various values of κ.

is in good agreement with the value derived by Sears. Knowing the value of Ω, it would be possible to evaluate the value of the integral that appears in Eq. (13) as a function of κ and compare it with the result that is obtained if the integral is solved numerically with an experimentally determined $g(r)$. This would give a test of the expression for the potential, but the computation is rather tedious and we have not attempted it.

The ratio of the observed first moment to the theoretical value was obtained by Randolph *et al.*[6] for liquid lead. They found that it was as large as 5 in certain regions of κ if multiple scattering was not corrected for. After making a rough correction for multiple scattering they obtained a ratio that was everywhere equal to 1 within 50%. The first-moment ratio obtained for liquid sodium by Randolph[32] came closer to 1 when multiple scattering was corrected for, but was still larger than 2 in certain regions of κ, and

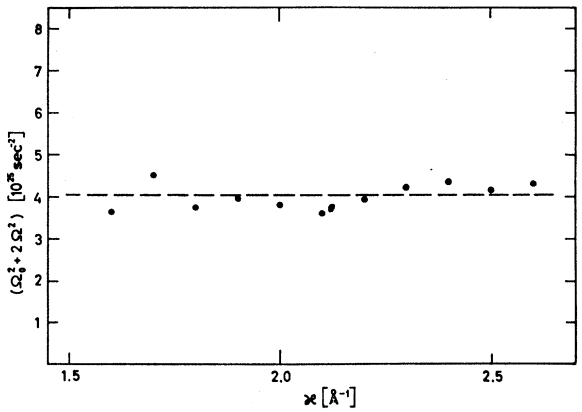

FIG. 18. Experimentally determined $\Omega_0^2+2\Omega^2$ at various values of κ.

[31] V. F. Sears, Proc. Phys. Soc. (London) **86**, 953 (1965).

[32] P. D. Randolph, Phys. Rev. **134**, A1238 (1964).

furthermore showed a strong dependence on κ and on temperature.

It was concluded in both of these experiments that the first moment is very sensitive to the presence of multiple scattering, and this probably applies to the other moments as well. The fact that the moments obtained in the present experiment were in reasonable agreement with the expected values is taken as a confirmation of our assumption that multiple scattering was not very serious in this case. This lends some confidence to the conclusions that were drawn from the comparisons of the cross section with various models and also to the values that were obtained for the characteristic frequencies from a direct consideration of the moments. It should be stressed, however, that the results that were obtained from the moments are significant in a qualitative sense only.

VI. CONCLUSIONS

Singwi's approach is shown to be a considerable improvement over the convolution approximation. A good over-all agreement with the experimental results is obtained with reasonable values of the parameters, but the model fails to explain the structure in the first diffraction peak. This structure, which is experimentally well established, can be understood if it is assumed that the liquid "lattice" can absorb momentum and if the polarization of the vibrations is taken into account. Egelstaff's model, which is based on these ideas, is in good agreement with the observations if it is assumed that the transverse phonons do not contribute to the intensity, at least not for $\omega > 3\times10^{12}$ sec^{-1}. The absence of transverse phonons at these frequencies does not necessarily mean that they do not exist for all values of q, but perhaps only that they have energies considerably lower than the longitudinal phonons. In the experiment on lead by Cocking,[5] it was observed that the transverse peak in the spectrum of the polycrystalline solid disappeared on melting. Larsson,[10] on the other hand, found that the spectrum from polycrystalline aluminum, which was shown to consist mainly of transverse phonons, remained almost unchanged on melting. Evidence obtained so far is thus controversial, and more work has to be done. Perhaps we should not expect that all liquids behave in a similar way in this respect. Some liquids may propagate high-frequency transverse vibrations, while other liquids do not.

The frequency spectrum was determined experimentally and compared with the curve obtained by Rahman. The results are in good qualitative agreement, and both curves have maxima close to the frequency that is predicted by the itinerant-oscillator model of Sears. Almost the same value was obtained for this characteristic frequency from a consideration of the moments of the scattering law.

An important result of this study is the observation of a dispersion law which is linear within the experimental errors and has a slope close to the known velocity of sound. The dispersion-law results are the same whether Singwi's or Egelstaff's model is used, and they are also in good agreement with an earlier determination in which a different technique of analysis was employed. Phonons were actually observed in the second zone, which is centered at the first peak of $S(\kappa)$, and we can therefore conclude that at least the first two Brillouin zones are defined in liquid argon. The same conclusion was earlier drawn from the studies on liquid aluminum[10] and recently also from studies on liquid lead.[6]

The delayed-convolution approximation was not subjected to a serious test, but was in good qualitative agreement with the observations in the region of ω and κ where a comparison was made. The delay that was used in this comparison was about 10^{-12} sec, which is the same as the value observed by Dasannacharya *et al.*[15] for the delay time before diffusion sets in. One may interpret this delay time as the lifetime of the initial configuration, which thus lives long enough to allow vibrations of frequencies 10^{12}–10^{13} sec^{-1} to develop. If we consider the coherence parameter R, which we estimated to be approx. 15 Å, as the spatial extension of such more or less ordered atomic arrangements, we find that the wave vectors of these vibrations must also be expected to be well defined.

ACKNOWLEDGMENTS

The authors are indebted to Dr. R. Pauli and Dr. N. Starfelt for their kind interest and encouragement during this work, and to L. Karlén for skillful technical assistance.